Hemorrhage of MRI and Immunohistochemical Panels Distinguish Secretory Carcinoma From Acinic Cell Carcinoma

Hiroko Kuwabara, MD 🄳; Kiyohito Yamamoto, MD; Tetsuya Terada, MD; Ryo Kawata, MD;
Toshitaka Nagao, MD; Yoshinobu Hirose, MD

Objectives: Secretory carcinoma (SC, mammary analogue secretory carcinoma) is a salivary gland tumor with ETV6-NTRK3 gene fusion, and its differential diagnosis includes acinic cell carcinoma (ACC). As hemorrhage is often seen in SC, we hypothesized that magnetic resonance imaging (MRI) and immunohistochemical analyses could distinguish SC from ACC.

Study Design: Retrospective study.

Methods: We used ETV6-NTRK3 gene fusion analyses to reclassify 19 parotid gland tumors that had previously been diagnosed as SC or ACC, and then investigated hemorrhage in both hematoxylin-eosin (H&E)-stained sections and MRIs, and immunohistochemical expression of S-100, mammaglobin, DOG1, and α-amylase.

Results: The 19 tumors were genetically reclassified into 11 (58%) SC and 8 (42%) ACC. Combined S-100 and mammaglobin were specific for SC; whereas DOG1 was specific for ACC, and α-amylase was expressed only in 4 ACC cases (50%). H&E staining showed hemorrhage with hemosiderin deposition in all SC cases, and T2-weighted MRI showed hypointense areas in all investigated SC cases, but not in ACC.

Conclusion: Hemorrhage with hemosiderin deposition is frequently present in SC, and hemorrhage findings in MRI and an immunohistochemical panels for S-100, mammaglobin and DOG1 can distinguish SC from ACC.

Key Words: Secretory carcinoma, acinic cell carcinoma, salivary gland, MRI, immunohistochemistry.

Level of Evidence: 3b

INTRODUCTION

Secretory carcinoma (SC), which is also called as mammary analogue secretory carcinoma, is a recently described salivary gland tumor that shares morphological similarities with SC of the breast. Both SCs are known to have a chromosomal translocation, t(12;15)(p13;q25), that creates an ETS variant gene 6 (ETV6) in chromosome 12 with the neurotrophin-3 receptor gene (NTRK3) kinase domain (ETV6-NTRK3) fusion, which encodes a chimeric tyrosine kinase.[1] Most cases of salivary gland SC have been categorized in the entity diagnosed previously as acinic cell carcinoma (ACC). Although both SC and ACC are typically indolent,[2] SC shows a slightly higher lymph node metastatic rate and aggression than ACC.[3,4] Genuine high-grade transformation has been reported in some SC cases.[5] With the

expansion of selective tyrosine kinase inhibitors, recognition of advanced-stage SC eventually has direct therapeutic relevance.[6] Therefore, distinguishing SC from ACC is important.

The molecular analysis of ETV6-NTRK3 gene fusion is the gold standard for discriminating between SC and ACC. However, this molecular technology is not readily available in a routine laboratory, whereas diagnosis based on radiological imaging with immunohistochemical panels are more practical. SC histologically and cytologically shows cholesterol cleft and hemosiderin deposition,[7] which suggests hemorrhage. ETV6-NTRK3 is potentially oncogenic and may have transforming activity in both epithelial and mesenchymal cells.[8] Tyrosine kinase is related to angiogenesis through vascular endothelial growth factor (VEGF).[9] Moreover, infantile fibrosarcoma and congenital mesoblastic nephroma with the ETV6-NTRK3 fusion product is usually macroscopically hemorrhagic.[10,11] Taken together, hemorrhage with hemosiderin deposition seems to be effective for separating SC from ACC, and we reviewed magnetic resonance imaging (MRI) findings, because MRI is the imaging modality of choice for evaluating hemorrhage and hemosiderin.[12] SC is immunohistochemically positive for S-100 protein and mammaglobin, and typically negative for DOG1, whereas ACC is positive for DOG1 and negative for mammaglobin.[3,13] In addition to these antibodies, we reviewed α-amylase positivity, because serous acinar cells containing zymogen granules are found in ACC, not in SC.

Here, we investigated the pathological and MRI features on hemorrhage, as well as immunohistochemical

findings of tumor cells, including α-amylase, to distinguish SC from ACC.

MATERIALS AND METHODS

Patients and Morphological Evaluation

This study retrospectively analyzed 19 patients who were diagnosed as having ACC or SC of the parotid gland at our hospital between April 2000 and August 2017. These cases were genetically reclassified into SC and ACC, and reviewed by histological, immunohistochemical, and MRI analyses. The study protocol was approved by the Osaka Medical College Ethics Committee. Tissue samples were routinely fixed in 10% buffered formalin, dehydrated in a graded ethanol series, and embedded in paraffin wax. Serial sections, 3 μm thick, were stained using hematoxylin-eosin (H&E) and immunohistochemistry agents. Hemorrhage and its related histopathological findings, such as hemosiderin deposition, cholesterol cleft, and cholesterol granuloma, were investigated in H&E-stained sections. Hemosiderin was confirmed by Prussian blue staining, and hemosiderin distribution was scored under magnification (x10) using an BX53 microscope (Olympus, Tokyo, Japan), as 0: no staining, 1: occasional staining with most fields negative, 2: focally abundant staining with most fields without staining, 3: focally abundant staining with most fields showing positive staining, 4: prominent staining throughout the section.[14] The Mann-Whitney U test was used to compare hemosiderin distribution scores between SC and ACC. $P < .05$ were considered significant.

ETV6-NTRK3 Fusion Gene Analysis

Total RNA was extracted from the paraffin embedded tissue and amplified as previously described.[15] The cDNA samples were then subjected to PCR, using the sense primer TEL971 (complementary to ETV6 with sequence 5′-ACCACATCATGGTC TCTGTCTCCC-3′) and the antisense primer TRKC1059 (complementary to NTRK3 with sequence 5′-CAGTTCTCGCTTCAG CACGATG-3′). Amplification of a 110-bp product of the ETV6-NTRK3 fusion transcript was carried out according to the method described by Bourgeois et al.[16] In all positive cases, the PCR fragments were directly sequenced using a Big Dye Terminator Sequence kit (Applied Biosystems, Foster City, CA, USA).

Radiological Evaluation

We reviewed available MRI images. T2-weighted images (T2WI) with hypointense spots were designed as hemorrhages with hemosiderin depositions.[12,17]

Immunohistochemistry

Immunostaining was performed using a BOND-MAX autoimmunostainer (Leica Microsystems, Wetzlar, Germany). Deparaffinized and rehydrated sections were subjected to endogenous peroxidase blocking. After heating in antigen unmasking solution, slides were incubated with one the following antibodies: S-100 protein (Dako, Santa Clara, CA, USA), mammaglobin (304-1A5, 1:100, Dako), DOG1 (SP31, 1:50, Thermo Scientific, Cheshire, UK) and α-amylase (1:50, Nordic Immunology, Tiburg, the Netherlands). Color development was carried out using 3,3′-diaminobenzidine tetrahydrochloride, and slides were counterstained with hematoxylin. Appropriate tissue sections were used as positive controls, and procedures without primary antibodies were used as negative controls.

RESULTS

Reclassification by Genetical Analyses

Reverse transcription-PCR (RT-PCR) analysis found 11 cases (58%) with ETV6-NTRK3 fusion genes (Fig. 1). Nucleotide sequencing of the RT-PCR fragments confirmed the presence of identical fusion. The clinical, histological, immunohistochemical and MRI features of SC and ACC patients are detailed in Tables I and II.

Clinical Information

Patients with SC were predominantly male (9 cases, 82%) whose mean age was 34 years (range: 14–63 years); whereas the ACC group was predominantly female (7 cases, 88%) whose mean age was 55 years old (range: 45–64 years). Clinical follow up ranged from 3 months to 17 years; all patients were alive. Local recurrence was seen in one patient with SC (9%) and two with ACC (25%). Lymph node metastasis was seen in one SC patient (9%); distant metastases were absent.

Macroscopic and Histological Findings

Nine patients with SC cases (82%) had cystic lesions with hemorrhage and necrotic tissue, and hemorrhage and related findings (such as hemosiderin deposition and cholesterol clefts) were present in all SC cases (Table I, Fig. 2A,B). Numerous cholesterol clefts surrounded by foreign body type giant cells and chronic inflammation were seen in one case (Fig. 2C). Tumor cells showed a mixture of papillary, microcystic, follicular, and solid patterns with eosinophilic secretions, and they had eosinophilic and vacuolated cytoplasm. The stroma of papillary structures was abundant in vessels (Fig. 2D). The ACC showed solid and focal cystic patterns (Table II), and histologically they revealed unequivocal serous acinar differentiation. Occasional or focal hemosiderin deposition was seen in 6 ACC cases
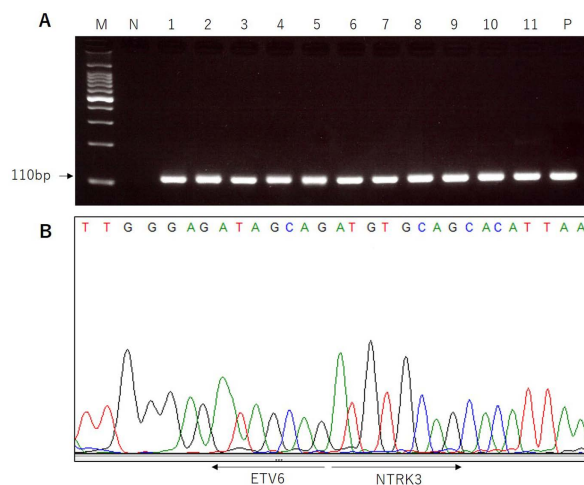

Fig. 1. (A) RT-PCR analysis shows amplification of ETV6-NTRK3 fusion transcripts in 11 cases. M: molecular weight marker, N: negative amplification control, P: positive amplification control. (B) Direct sequencing of amplified RT-PCR product confirms the presence of ETV6-NTRK3 rearrangement.

	Sex/age	pTN	Treatment	Macroscopic and histopathological findings	Hemorrhage	Hemosiderin distribution	Hypointense in T2WI	S-100	MG	DOG1	α-Amylase
1	M/25	T2N0	PP,LND	cyst, solid, cholesterol clefts	(+)	3	ND	(+)	(+)	(−)	(−)
2	M/52	T2N0	PP,LND	solid	(+)	3	ND	(+)	(+)	(−)	(−)
3	M/32	T2N2	PP,LND	cyst, solid, cholesterol clefts	(+)	2	ND	(+)	(+)	(−)	(−)
4	F/14	T2N0	PP	cyst, solid	(+)	3	(+)	(+)	(+)	(−)	(−)
5	M/20	T2N0	PP,LND,RT	cyst, solid, cholesterol granuloma	(+)	4	(+)	(+)	(+)	(−)	(−)
6	M/22	T2N0	PP,LND	solid, psammoma body, cholesterol clefts	(+)	3	(+)	(+)	(+)	(−)	(−)
7	M/23	T1N0	MR	cyst, solid	(+)	3	(+)	(+)	(+)	(−)	(−)
8	M/49	T2N0	MR,LND	cyst, solid, cholesterol clefts, hemorrhage	(+)	4	(+)	(+)	(+)	(−)	(−)
9	M/63	T3N0	MR,LND,RT	cyst, solid, cholesterol clefts	(+)	2	(+)	(+)	(+)	(−)	(−)
10	F/15	T2N0	MR	cyst, solid, cholesterol clefts	(+)	3	(+)	(+)	(+)	(−)	(−)
11	M/61	T2N0	PP,LND,RT	cyst, solid, cholesterol clefts	(+)	3	(+)	(+)	(−)	(−)	(−)

MR = mass resection; RT = radiation therapy; PP = partial parotidectomy; LND = lymph node dissection; ND = not done; MG = mammaglobin

(75%), but a hemosiderin deposition area in ACC was less than for SC ($P < .001$), and cholesterol clefts and granulomas were absent.

MRI Findings

All eight SC patients showed hypointense lesion in T2WI, which suggest hemorrhages with hemosiderin deposition. One case showed a shading sign with progressive layered signal loss (Fig. 3). In contrast, all six ACC patients had no hypointensity lesion in T2WI (Fig. 4).

Immunohistochemistry

SC cells were positive for S100, mammaglobin and negative for DOG1 and α-amylase, except for one case (Table I; Fig. 5). DOG1 was expressed in apical-luminal region of all ACC cases, while S100 and mammaglobin

were negative (Fig. 6). α-amylase positivity was seen in four ACC cases (50%).

DISCUSSION

The present study shows that SC and ACC are different disease entities, as shown from clinical, MRI, and immunohistochemical findings. Males predominated in SC and females in ACC, which conforms with a previous study.[4] Our cohort had two pediatric SC cases (14 and 15 years old). To our knowledge, 16 cases of pediatric SC have been reported in the literature,[18,19] and SC should be included in differential diagnosis of pediatric salivary gland tumors.

This study is the first histological and MRI analysis of hemorrhage in SC. On MRI, T2WI hypointense lesions were characteristic of SC, which seemed to correspond to cystic lesions with hemosiderin depositions following hemorrhage. Although hemosiderin was seen in six ACC

	Sex/age	pTN	Treatment	Macroscopic and histopathological findings	Hemorrhage	Hemosiderin deposition	Hypointense in T2WI	S-100	MG	DOG1	α-Amylase
1	F/51	T2N0	TP,LND	solid, cyst	(+)	1	ND	(−)	(−)	(+)	(+)
2	F/45	T1N0	PP,LND	solid	(−)	0	(−)	(−)	(−)	(+)	(+)
3	F/64	T3N0	PP,LND	solid	(−)	0	ND	(−)	(−)	(+)	(−)
4	F/64	T4aN0	PP,LND,RT	solid, cyst	(−)	1	(−)	(−)	(−)	(+)	(−)
5	F/61	T2N0	MR,RT	solid	(+)	2	(−)	(−)	(−)	(+)	(+)
6	F/60	T1N0	MR	solid	(−)	1	(−)	(−)	(−)	(+)	(+)
7	F/46	T1N0	MR,LND	solid, cyst	(−)	1	(−)	(−)	(−)	(+)	(−)
8	M/53	T2N0	MR,LND	solid, cyst	(+)	2	(−)	(−)	(−)	(+)	(−)

MG = mammaglobin; ND = not done; MR = mass resection; R = : radiation therapy; TP = total parotidectomy; PP = partial parodidectomy; LND = lymph node dissection
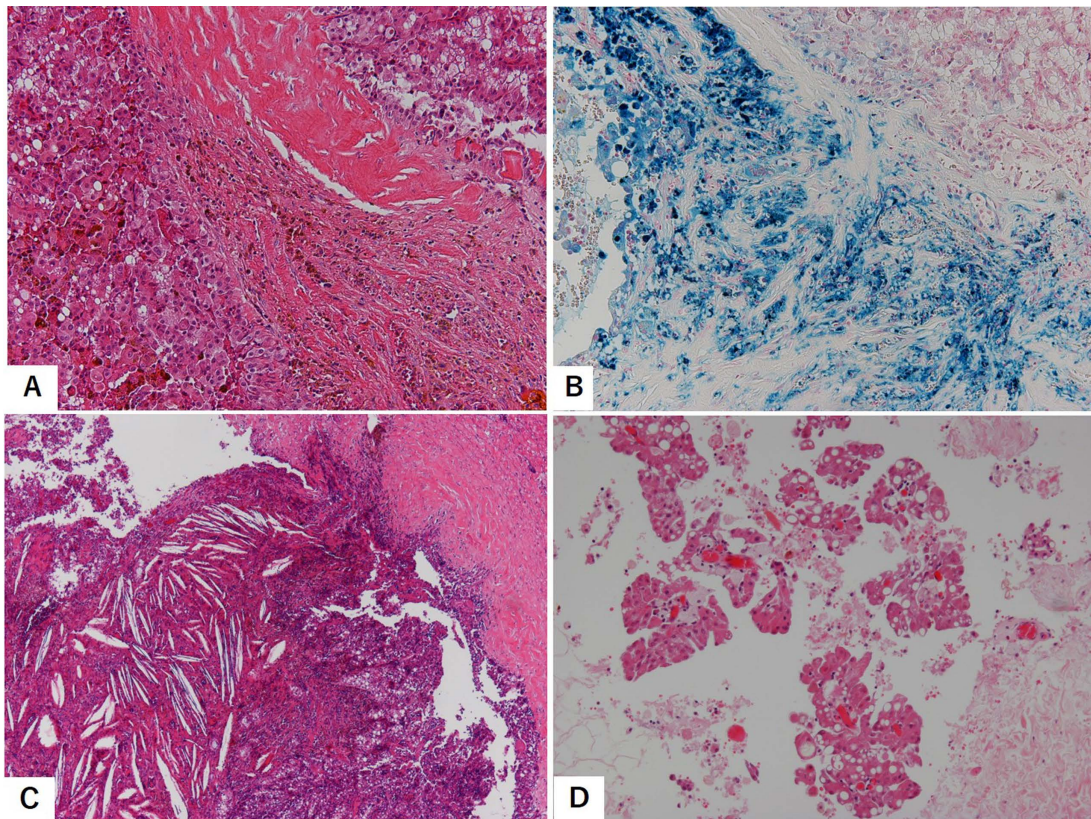
Fig. 2. Representative images of secretory carcinoma. Hemosiderin deposition (A) (H&E, original magnification X10), Prussian blue staining (B) (original magnification X10), cholesterol granuloma (C) (H&E, original magnification X2) and papillary growth with abundant vessels (D) (H&E, original magnification X2).
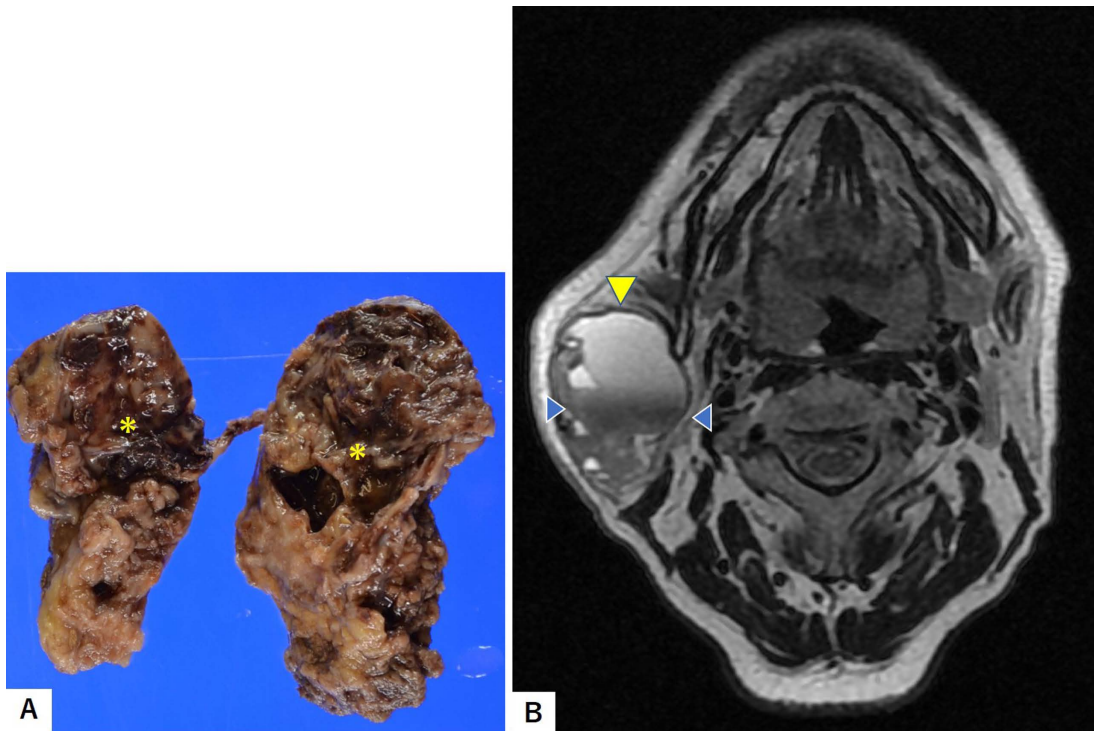

Fig. 3. Macroscopic figure (A) and T2-weighted MRI (B) of secretory carcinoma. (A) Cystic lesion with bleeding (yellow asterisks), (B) the shading sign with hypointense lesion in the cystic bottom (blue arrowheads). Tumor (yellow arrowhead). MRI = magnetic resonance imaging.

Fig. 4. Macroscopic figure (A) and T2-weighted MRI (B) of acinic cell carcinoma. Tumor (A: yellow asterisks, B: yellow arrowhead). MRI = magnetic resonance imaging.
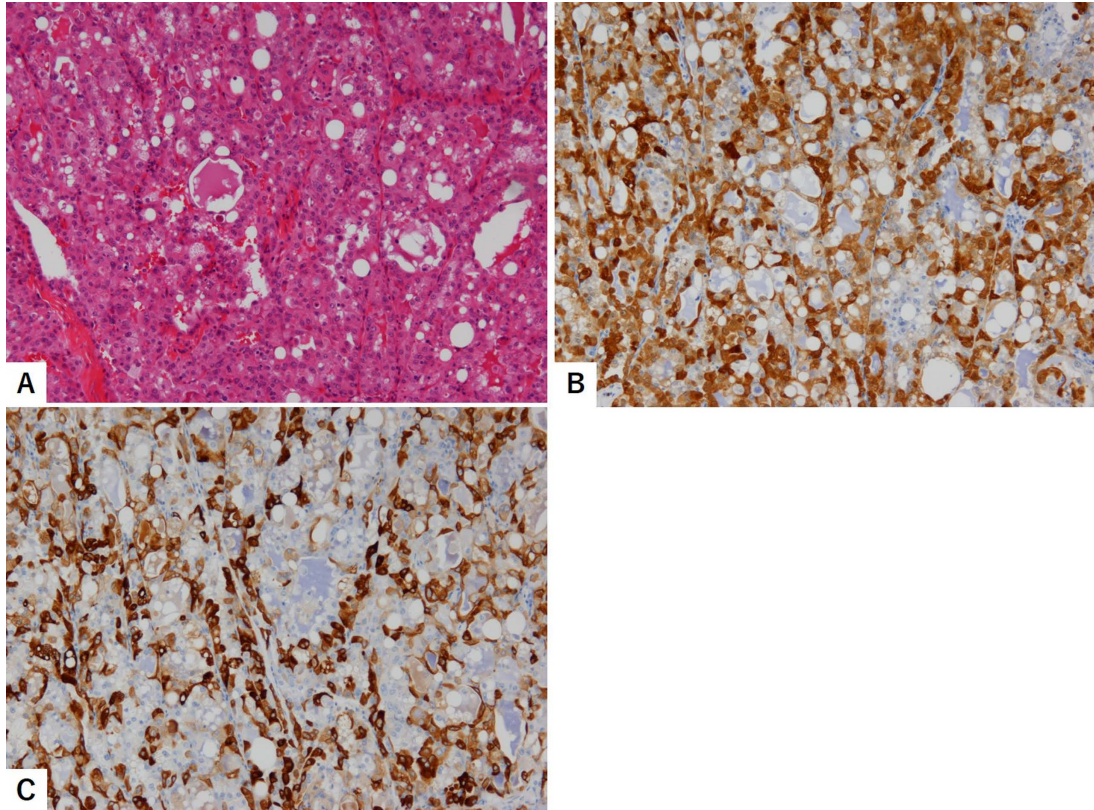

Fig. 5. Representative immunohistochemical images of secretory carcinoma. (A) Papillary and microcystic proliferation (H&E, original magnification X10). Immunohistochemical staining for S-100 (B) and mammaglobin (C) (original magnification X10).
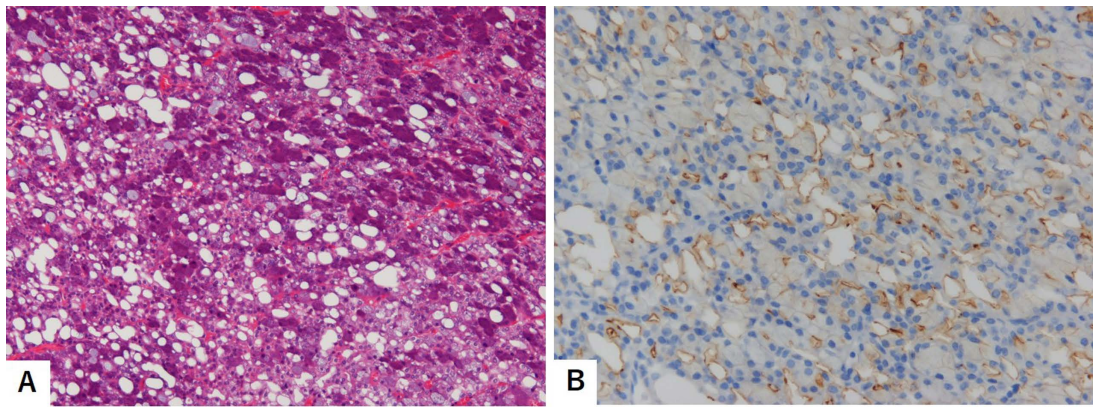
Fig. 6. Representaive immunohistochemical images of acinic cell carcinoma. (A) Tumor cells with acinic cell differentiation (H&E, original magnification ×10). (B) Immunohistochemical staining for DOG1 (orginal magnification ×20).

cases, those areas were focal and MRI revealed no hypointense areas. Hemorrhage biochemically converts oxyhemoglobin, deoxyhemoglobin, methemoglobin, and hemosiderin. MRI is useful for detecting hemosiderin, and chronic cerebral hemorrhage with hemosiderin deposition is shown by hypointensity on T2WI.[12] The shading sign seen in one SC case is a MRI feature of endometrioma, which shows hemorrhage and hemosiderin deposition.[20] In the fine needle aspiration cytology of SC, the hemosiderin-laden histiocyte-rich background is a characteristic.[7] MRI seems to be useful for the preoperative diagnosis of SC, in addition to aspiration cytology. Recently, T2 star-weighted imaging, which is useful for detecting hemosiderin, has been developed, and it improves sensitivity for detecting intracerebral hemorrhage and endometrioma.[21,22] T2 star-weighted imaging may be available also for salivary gland tumors. The reason why SC hemorrhages so frequently is not clear, but we speculate that ETV6-NTRK3 fusion gene has an important role. The product of this fusion gene induces angiogenesis through VEGF,[9] and VEGF overexpression is known to induce tumor-related cyst formation, peritumoral edema formation and hemorrhage.[23] Furthermore, the papillary stromal components in SC were abundant in vessels, and the papillary formation is associated with angiogenesis in some tumors.[24] Our preliminary examination shows more abundant neovascularization in SC than in ACC, and the angiogenetic process may be crucial in SC.

Another important clue for distinguishing SC from ACC is an immunohistochemical analysis.[25] In this study, the best agreements with ETV6-NTRK3 positive RT-PCR analyses were immunohistochemical panels that stained S-100+, mammaglobin+, and DOG1−, as seen in a previous report.[26] Serous acinar cells that contained zymogen granules are specific to ACC, but only half of the ACC were α-amylase positive. However, the apical-luminal pattern of DOG1 was seen in all ACC cases, and this staining pattern of DOG1, not α-amylase, is important for distinguishing ACC from SC.

The ETV6-NTRK3 translocation forms a chimeric tyrosine kinase, which is a potential therapeutic target of SC. Infantile fibrosarcoma, which is a rare myofibroblastic/fibroblastic tumor and carries ETV6-NTRK3 translocation, had a rapid response to selective tropomyosin-related kinase inhibitor LOXO-101.[27] The correct diagnosis of SC is necessary for appropriate therapy, particularly when a high-grade transformation occurs.[6] In addition, SC shows a slightly higher lymph node metastatic rate,[3,4] and MRI findings and immunohistochemical panels of SC are useful for managing the patient.

CONCLUSION

Hemorrhage with hemosiderin deposition and an immunohistochemical panel of S-100, mammaglobin and DOG1 distinguish SC from ACC. In addition, MRI is useful for evaluating SC hemorrhage.

BIBLIOGRAPHY

1. Skalova A, Vanecek T, Sima R, et al. Mammary analogue secretory carcinoma of salivary glands, containing the ETV6-NTRK3 fusion gene: a hitherto undescribed salivary gland tumor entity. *Am J Surg Pathol* 2010;34:599–608.
2. Griffith C, Seethala R, Chiosea SI. Mammary analogue secretory carcinoma: a new twist to the diagnostic dilemma of zymogen granule poor acinic cell carcinoma. *Virchow Arch* 2011;459:117–118.
3. El-Naggar AK, Chan JKC, Grandis JR, Takata T, Slootweg PJ. WHO Classification of Head and Neck Tumours. Lyon: IARC; 2017.
4. Chiosea SI, Griffith C, Assaad A, Seethala RR. Clinicopathological characterization of mammary analogue secretory carcinoma of salivary glands. *Histopathology* 2012;61:387–394.
5. Skalova A, Vanecek T, Majewska H, et al. Mammary analogue secretory carcinoma of salivary glands with high-grade transformation: Report of 3 cases with the ETV6-NTRK3 gene fusion and analysis of TP53, β-Catenin, EGFR, and CCND1 genes. *Am J Surg Pathol* 2014;38:23–33.
6. Baghai F, Yazdani F, Etebarian A, Garajei A, Skalova A. Clinicopathologic and molecular characterization of mammary analogue secretory carcinoma of salivary gland origin. *Pathol Res Pract* 2017;213:1112–1118.
7. Higuchi K, Urano M, Takahashi R, et al. Cytological features of mammary analogue secretory carcinoma of salivary gland: Fine-needle aspiration of seven cases. *Diagn Cytopathol* 2014;42:846–855.
8. Lannon CL, Soresen PH. TEV6-NTRK3: a chimeric protein tyrosine kinase with transformation activity in multiple cell lineages. *Semin Cancer Biol* 2005;15:215–223.

9. Aparicio LM, Fernandez IP, Cassinello J. Tyrosine kinase inhibitors reprogramming immunity in renal cell carcinoma: rethinking cancer immunotherapy. *Clin Transl Oncol* 2017;19:1175–1182.

10. Fletcher CDM, Bridge JA, Hogendoorn PCW, Mertens F. WHO Classification of Tumours of Soft Tissue and Bone. Lyon: IARC; 2013.

11. Moch H, Humphrey PA, Ulbright TM, Reuter VE. WHO Classification of Tumours of the Urinary System and Male Genital Organs. Lyon: IARC; 2015.

12. Grossman R, Gomori J, Goldberg HI, et al. MR imaging of hemorrhagic conditions of the head and neck. *RadioGraphics* 1988;8:441–454.

13. Chenevert J, Duvvuri U, Chiosea S, et al. DOG1: a novel marker of salivary acinar and intercalated duct differentiation. *Mod Pathol* 2012;25:919–929.

14. Turkmen IN, Eren F, Akgoz S, et al. The importance of hemosiderin deposition in the infant brain: an autopsy study. *Hippokratia* 2015;19:164–171.

15. Tsuji S, Hisaoka M, Morimitsu Y, et al. Detection of SYT-SSX fusion transcripts in synovial sarcoma by reverse transcription polymerase chain reaction using archival paraffin-embedded tissues. *Am J Pathol* 1998;153:1807–1812.

16. Bourgeois JM, Knezevich SR, Mathers JA, Sorensen PH. Molecular detection of the ETV6-NTRK3 gene fusion differentiates congenital fibrosarcoma from other childhood spindle cell tumors. *Am J Surg Pathol* 2000;24:937–946.

17. Soo Lee Y, Tae Kwon S, Ok Kim J, Seok Choi E. Serial MR imaging of intramuscular hematoma: experimental study in a rat model with the pathologic correlation. *Korean J Radiol* 2011;12:66–77.

18. Ngouajio AL, Drejet SM, Phillips DR, Summerlin DJ, Dahl JP. A systemic review including an additional pediatric case report: Pediatric cases of mammary analogue secretory carcinoma. *Int J Pediatric Otorhinolaryngol* 2017;100:187–193.

19. Xu B, Aneja A, Ghossein R, Katabi N. Salivary gland epithelial neoplasms in pediatric population: a single-institute experience with a focus on the histologic spectrum and clinical outcome. *Hum Pathol* 2017;67:37–44.

20. Dias JL, Veloso Gomes F, Lucas R, Cunha TM. The shading sign: is it exclusive of endometriomas? *Abdom Imaging* 2015;40:2566–2572.

21. Takahashi N, Yoshino O, Maeda E, et al. Usefulness of T2 star-weighted imaging in ovarian cysts and tumors. *J Obstet Gynaecol Res* 2016;42:1336–1342.

22. Mule S, Soize S, Benaissa A, Portefaix C, Pierot L. Detection of aneurysmal subarachnoid hemorrhage 3 months after initial bleeding: evaluation of T2* and FLAIR MR sequences at 3 T in comparison with initial non-enhanced CT as a gold standard. *J Neurointerv Surg* 2016;8:813–818.

23. Kim YJ, Kim CH, Cheong JH, Kim JM. Relationship between expression of vascular endothelial growth factor and intratumoral hemorrhage in human pituitary adenomas. *Tumori* 2011;97:639–646.

24. Diaz-Flores L, Gutierrez R, Garcia MDP, Saez FJ, Diaz-Flores L Jr, Madrid JF. Piecemeal mechanism combining sprouting and intussusceptive angiogenesis in intravenous papillary formation induced by PGE2 and Glycerol. *Anat Rec* 2017;300:1781–1792.

25. Urano M, Nagao T, Miyabe S, et al. Characterization of mammary analogue secretory carcinoma of the salivary gland: discrimination from its mimics by the presence of the ETV6-NTRK3 translocation and novel surrogate markers. *Hum Pathol* 2015;46:94–103.

26. Pinto A, Nose V, Rojas C, Fan YS, Gomez-Fernandez C. Searching for mammary analogue secretory carcinoma of salivary gland among its mimics. *Mod Pathol* 2014;27:30–37.

27. Nagasubramanian R, Wei J, Gordon P, et al. Infantile fibrosarcoma with NTRK3-ETV6 fusion successfully treated with the tropomyosin-related kinase inhibitor LOXO-101. *Pediatr Blood Cancer* 2016;63:1468–1470.